

# The Eddy Experiment: GNSS-R specularometry for directional sea-roughness retrieval from low altitude aircraft

O. Germain, G. Ruffini, F. Soulat, M. Caparrini,<sup>1</sup> B. Chapron<sup>2</sup> and P. Silvestrin<sup>3</sup>

We report on the retrieval of directional sea surface roughness, in terms of its full directional mean square slope (including direction and isotropy), from Global Navigation Satellite System Reflections (GNSS-R) Delay-Doppler-Map (DDM) data collected during an experimental flight at 1 km altitude. This study emphasizes the utilization of the entire DDM to more precisely infer ocean roughness directional parameters. In particular, we argue that the DDM exhibits the impact of both roughness and scatterer velocity. Obtained estimates are analyzed and compared to co-located Jason-1 measurements, ECMWF numerical weather model outputs and optical data.

## 1. Introduction

Several GNSS constellations and augmentation systems are presently operational or under development, including the pioneering US Global Positioning System (GPS) and the forthcoming European system, Galileo. These all-weather, long-term, stable and precise L-band signals can be used for bistatic remote sensing of the ocean surface and beyond, an emerging concept known as GNSS-R.

<sup>1</sup>Starlab, C. de l'Observatori Fabra s/n, 08035 Barcelona, Spain, <http://starlab.es>

<sup>2</sup>Ifremer, Technopôle de Brest-Iroise BP 70, 2920 Plouzané, France, <http://ifremer.fr>

<sup>3</sup>ESA/ESTEC, Keplerlaan 1, 2200 Noordwijk, The Netherlands, <http://esa.int>

Copyright 2018 by the American Geophysical Union. 0094-8276/18/\$5.00

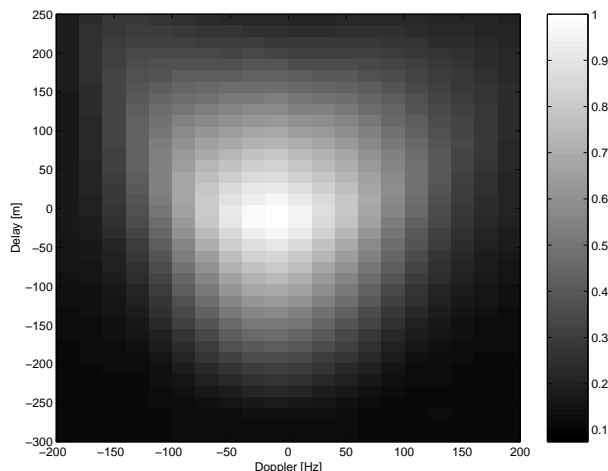


Figure 1. Example of GPS-R Delay-Doppler Map.

Among several applications, two have been emphasized by the community: sea-surface altimetry (see *Ruffini et al.* [2004] and references therein) and sea-surface “specularometry” (a term discussed below), related to the statistical properties of sea surface gravity wave slopes. Although this paper addresses the latter, we note the intrinsic capability of GNSS-R for providing long term co-located measurements of both surface roughness and sea level with high spatial and temporal resolution. As recently demonstrated with scatterometer measurements (*Chelton et al.* [2004]), such a capability would help to better quantify the relationship of velocities in the upper ocean (driven by wind stress forcing) with surface height dynamics.

Thanks to its passive multistatic character, GNSS-R clearly holds the potential to provide an unprecedented spatio-temporal sampling of the ocean surface. The expected high spatial and temporal measurements can certainly serve operational applications. For instance, and to follow successful scatterometer measurements, GNSS-R can complement ocean winds and wave models. Being rain immune, such new data could help quantify atmosphere-ocean coupling, including momentum and energy fluxes under extreme conditions for hurricane modeling. Many other scientific applications can be cited, such as sea surface breaking/whitcapping and gas exchange global characterization, important ingredients for understanding the ocean’s biogeochemical response to, and its influence on, climate change. Indeed, a very promising approach to quantify CO<sub>2</sub> flux is to better assess the surface fractional area, which is readily measurable from surface slope measurements (*Watson et al.* [1999]). In that case, GNSS-R can provide a more direct measurement to extract gravity surface slope statistical properties and to quantify the role of the ocean in taking up increases of CO<sub>2</sub>.

In addition, L-band sea surface roughness data can be used to support L-band radiometric missions, such as SMOS (Soil Moisture and Ocean Salinity) and AQUARIUS, to both quantify and efficiently separate roughness and salinity contributions to L-band radiometric brightness measurements.

Inferring sea roughness from GNSS-R data requires (i) a parametric description of the sea surface, (ii) an electromagnetic and instrument model for sea-surface scattering at L-band and (iii) the choice of a GNSS-R data product to be inverted. There is quite an agreement on the two first aspects in the literature. It has been recognized that the scattering of GNSS signals can be approximated by an *effective* Geometric Optics model, where the fundamental physical process is the scattering from facet-like surface elements. This is the reason for the use of the term “specularometry” here, which stems from the Latin word for mirror, *speculo*: the detected GNSS-R return is dominated by the statistics of facet slopes and their curvatures at scales larger than the electromagnetic wavelength ( $\lambda$ ).

Under a Gaussian assumption, three parameters fully define the detected L-band sea surface slope probability distribution (PDF). These parameters are encapsulated by the directional mean square slope,  $DMSS_\lambda$ , a symmetric tensor which results from the integration of the ocean energy spectrum at wavelengths larger than  $\lambda$ , and which characterizes the ellipsoidal shape of the slope PDF.

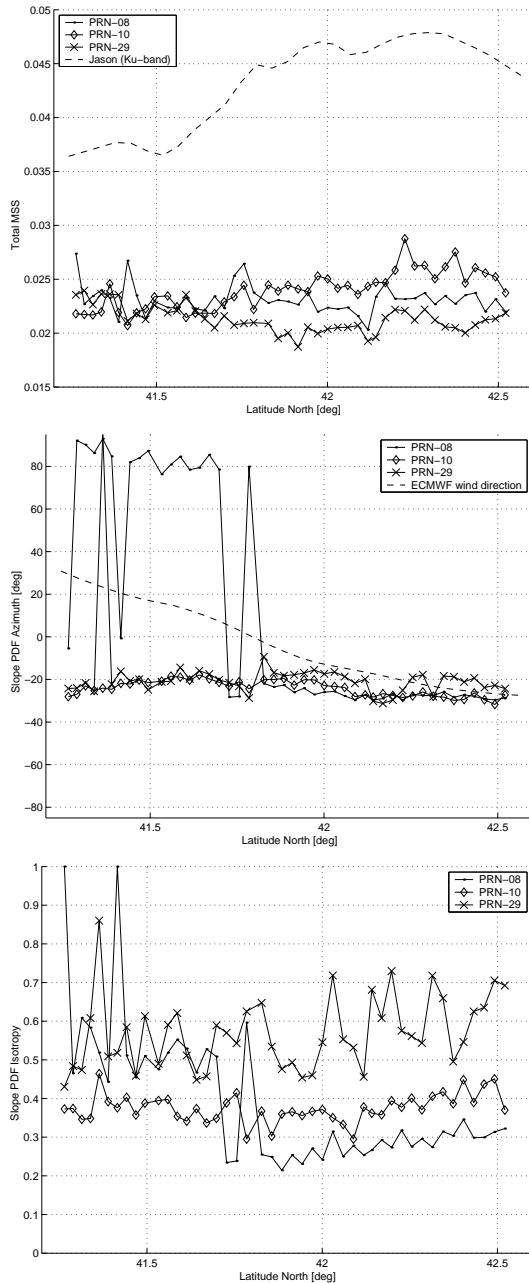


**Figure 2.**  $DMSS_\lambda$  estimation with the DDM least-square inversion approach, along the descending (North to South) track—MSS top, SPA middle and SPI bottom. The total MSS (Ku-Band) measured by Jason-1 and the ECMWF wind direction are also shown for comparison.

It is important to note that  $DMSS_\lambda$  has rarely been emphasized as the geophysical parameter of interest in the literature. Instead, most authors link sea roughness to the near surface wind vector, which is thought to be more useful for oceanographic and meteorological users. Unfortunately, this is somewhat misleading, as the relationship between surface wind and roughness is not one-to-one and requires an additional modeling layer. The connection between  $DMSS_\lambda$  and wind is affected by other factors (e.g., swell, fetch and degree of maturity), as is well known in the altimeter community (see *Gourrion et al.* [2002]).

Moreover, the product traditionally used for inversion in GNSS-R specularometry is the 1D delay waveform of the reflected signal amplitude, from which the wind speed is inferred assuming an isotropic slope PDF (see, e.g., *Garrison et al.* [1998, 2002] *Komjathy et al.* [2000], or *Cardellach et al.* [2003]). Attempts have also been made to estimate the wind direction by fixing the PDF isotropy to some theoretical value (around 0.7) and using at least two satellites reflections with different azimuths (see, e.g., *Zuffada et al.* [2000], *Armatys et al.* [2000] and *Garrison et al.* [2003]).

Here, we will work with a product of higher information content: the 2D DDM of the reflected signal amplitude. As proposed in *Ruffini et al.* [2000], the provision of an extra dimension opens the possibility of performing a robust estimation of all the  $DMSS_\lambda$  parameters through the direct fitting/estimation of the entire DDM. In *Elfouhaily et al.* [2002], a first order approximation for inversion was proposed.

The full DDM-inversion technique proposed in *Ruffini et al.* [2000] is used for the first time here to analyze GNSS-R data collected during the Eddy Experiment. This campaign and the altimetric data analysis is reported elsewhere (*Ruffini et al.* [2004] and *Soulat* [2003]), and is only briefly described in Section 2. The retrieval methodology relies on a least-squares fit of the specularometric model, as discussed in the third section. In the fourth section, results are compared to ancillary data (Jason-1 radar altimeter, ECMWF numerical weather model, optical data). Finally, another important outcome of the exhaustive exploitation of the information contained in the DDM product is related to the expected mean sea surface motion. We evidence that a small part of the Doppler spread can be attributed to the mean “scatterer velocity”, i.e., the rapid motion of the  $\lambda$  (or larger) sized sea-surface facets that contribute the most to the detected signals.

## 2. Data collection and pre-processing

The data set (i.e., the recorded direct and reflected GPS signals together with the aircraft kinematic data) was gathered during an airborne campaign carried out in September 2002. The aircraft overflew the Mediterranean Sea, off the coast of Catalonia (Spain), northwards from the city of Barcelona for about 150 km at 1000 m altitude and 45-75 m/s speed. The area is crossed by the ground track #187 of the Jason-1 radar altimeter, which the aircraft overflew during the satellite overpass for precise comparison. The track was overflown twice: the first time during the ascending pass (from South to North) at low speed (45-60 m/s) and the second during the descending pass (from North to South) at a faster speed (65-75 m/s) due to wind. The time shift between the two passes over a same point on the track ranged from 45 min to 2h 15 min. During the ascending pass, PRNs 08, 10 and 24 were visible with elevations spanning  $30^\circ$  to  $85^\circ$  while PRNs 08, 10 and 29 were visible during the descending track with elevations between  $40^\circ$  and  $75^\circ$ . The configuration of this test flight was not optimized for specularometry: from such low altitude, the sea-surface reflective area is essentially limited by the PRN C/A code, and the glistening zone is coarsely Delay-Doppler mapped.

The raw GPS signals were acquired with a modified TurboRogue receiver, sampled at 20.456 MHz and pre-processed with a dedicated software composed of two sub-units fed with the direct and reflected signals. Correlations were computed at 81 delay lags while the Doppler dimension spanned -200 to 200 Hz with a step of 20 Hz. The coherent/incoherent integration times were respectively set to 20 ms and 10 s, meaning that the averaged DDM were produced at the rate of 0.1 Hz after summation of 500 incoherent looks (see Figure 1 for a sample DDM).

### 3. Speculometric model and DDM inversion

Following *Zavorotny et al.* [2000], the link between the DDM mean power at delay-Doppler  $P(\tau, f)$  and the effective L-band sea-surface slope PDF,  $\mathcal{P}(s_x, s_y)$ , is given by

$$P(\tau, f) = \int dx dy \frac{G_r}{R_t^2 R_r^2} \cdot \frac{q^4}{q_z^4} \cdot \mathcal{P}\left(\frac{-q_x}{q_z}, \frac{-q_y}{q_z}\right) \cdot \chi^2[\tau_m(x, y) - \tau_c - \tau, f_m(x, y) - f_c - f], \quad (1)$$

where  $G_r$  is the receiver antenna pattern,  $R_t$  and  $R_r$  the distances from generic point on sea-surface to transmitter and receiver,  $(q_x, q_y, q_z)$  the scattering vector,  $\chi$  the Woodward Ambiguity Function (WAF),  $\tau_m(x, y)$  and  $f_m(x, y)$  the delay-Doppler coordinates on the sea-surface and  $(\tau_c, f_c)$  the delay/Doppler offset of the geometric specular-point with respect to the direct signal (the DDM “center”). Accounting for the receiver mean thermal noise  $P_N$  and including a scaling parameter  $\alpha$ , the mean amplitude of the DDM can be written as  $A(\tau, f) = \sqrt{\alpha P(\tau, f) + P_N}$ . As discussed above,  $\mathcal{P}$  is described by the  $\text{DMSS}_\lambda$  parameter set, which defines an elliptic quadratic form in the 2D space of facet slopes. Mean-square slopes along major and minor principal axes are often called MSS up-wind ( $mss_u$ ) and MSS cross-wind ( $mss_c$ ) respectively. In the following, we will refer to the Total MSS ( $\text{MSS}_{tot} = 2\sqrt{mss_u \cdot mss_c}$ , proportional to the ellipse area and directly related to nadir  $\sigma^\circ$ ), the Slope PDF azimuth (SPA, the direction of semi-major axis with respect to North) and the Slope PDF Isotropy (SPI, equal to  $mss_c/mss_u$ ).

The inversion was performed through minimization of the mean square difference between model and data DDMs. Numerical optimization was carried out by a steepest-slope-descent algorithm with a Levenberg-Marquardt type adjustment. The main difficulty stemmed from the presence of several nuisance parameters in the forward model (mainly  $\tau_c$  and  $f_c$  but also  $\alpha$ ). The DDM centers were affected by the aircraft trajectory (altitude and vertical velocity) to first order but also by geophysical parameters (such as sea level). They needed to be accurately known in order to estimate  $\text{DMSS}_\lambda$ . For this reason, the  $\text{DMSS}_\lambda$  and nuisance parameters were jointly estimated in an iterative manner.

### 4. Results and analysis

The values of  $\text{DMSS}_\lambda$  estimated along the descending track of the flight are shown on Figure 2. The top plot illustrates the variations of Total MSS. The inter-PRN consistency is reasonable in the southern part of the track but worsens slightly in the northern part. For comparison, the total MSS in Ku-band was derived from the Jason-1  $\sigma^0$  collocated measurements at 1 Hz sampling (7 km) and 20 km resolution. The Jason-1 MSS was obtained through the simple relationship  $\text{MSS} = \kappa/\sigma^0$ ,  $\kappa$  being the effective (empirical) Fresnel coefficient, here set to 0.45. As expected, we observed that the level and dynamic of MSS decreased with longer wavelength (from 2 cm in Ku-band to 19 cm in L-band). The lower dynamic of L-band MSS impeded any clear trend comparison, although the measurements of PRN-10 seem in good agreement with Jason-1. The Jason-1 wind speed, derived from both the Ku-band  $\sigma^0$  and the significant wave height (of about 2 m), ranged from 9 to 13 m/s along the track. Translating this wind speed into L-band MSS through the spectrum of *Elfouhaily et al.* [1997] yields values between 0.0220 and 0.0255, in-line with GNSS-R results. However, we must emphasize that the assumption of a wind-driven spectrum was not really warranted during the campaign.

SPA estimation results are presented on the middle plot. The inter-PRN consistency is here very satisfying, and the

apparent discrepancy in the southern part of the track can be explained as a degenerate solution of the estimation problem. Indeed, the inversion of DDM for the SPA is degenerate in at least two cases: when the transmitter is at zenith or when the receiver moves towards the transmitter. In these scenarios, the Delay-Doppler lines mapping the glistening zone are fully symmetric around the receiver direction and it becomes impossible to distinguish a slope PDF from its mirror image about the receiver direction. This effect is clearly observed here where the two found SPA ( $-20^\circ$  and  $80^\circ$ ) are indeed symmetric around the aircraft heading direction ( $30^\circ$ ). In this part of the track, the azimuth of PRN-08 is about  $50^\circ$ , almost aligned with the aircraft heading direction. In the northern part of the track, the estimated SPA matches very well with the wind direction provided by ECMWF. In the southern part, the mismatch reaches up to  $50^\circ$ . However, we underline that surface wind is not the only element driving SPA and that swell is likely to have contributed.

Finally, the bottom plot shows the SPI variations along the track. The reflected signals are strongly directional. The wind-driven spectrum of *Elfouhaily et al.* [1997] for a mature sea predicts a SPI value around 0.65, largely insensitive to wind speed. The apparent significant departure from this reference value is a probable signature of an under-developed sea with the presence of swell. However, the relatively poor consistency among PRN remains an issue to clarify: further work is needed to validate the accuracy of these SPI estimates and to better understand the potential information (and possible applicability constraints) of this product.

As a second and new outcome of this analysis, we now discuss the signature of “scatterer velocity” in the data, i.e., the signature of fastly moving sea-surface facets with size (curvature) larger than  $\sim 20$  cm. Such a signature can be detected when comparing the total MSS along the ascending and descending tracks, as estimated by the least-squares approach: a drastic discrepancy (up to 33%) was observed for two passes shifted by less than hour over the same track point.

Multipath effects could conceivably lead to a Doppler width modulation. However, some azimuth dependence should have been observed and was not. Another possible cause could be a changing aircraft attitude between ascending and descending tracks, but the aircraft roll and pitch

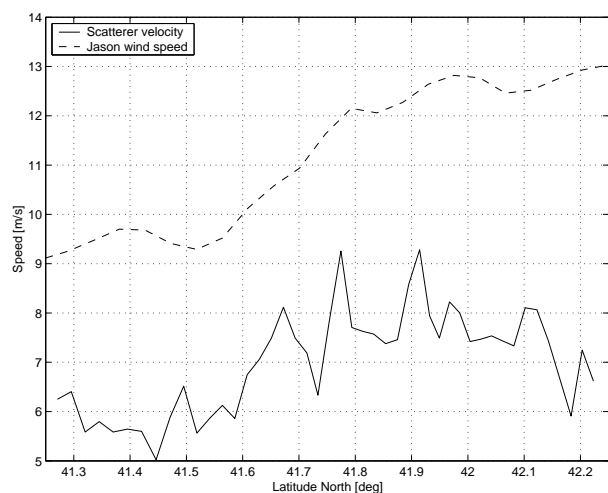


**Figure 3.** Average scatterer velocity obtained when assuming a perfect match of ascending/descending MSS and the first order MSS model. It correlates fairly well with wind speed and the observed swell from optical data.

values were checked to be nominal along both tracks. Moreover, a change in yaw would slightly impact the antenna pattern ground projection but would translate only into a Doppler bandwidth cut and never a broadening. We concluded that the most likely explanation was of geophysical origin: the Doppler spectral width had been modulated by the overall sea surface dynamics as detected from the mean specular facet motion. While the inversion approach assumed a still surface, the relative velocity between receiver and scatterer should be taken into account for proper DDM inversion. At high receiver velocities this assumption is fine because the scatterer velocity impact will not be significant. At low speeds, however, scatterer velocity becomes relevant. This analysis is consistent with the fact that the MSS estimated in the ascending track (slower aircraft speed, from 45 to 60 m/s) showed abnormal high values compared to the ones estimated during the ascending track (faster speed, from 65 to 75 m/s).

In order to test this idea in a simple manner, we used the results in *Elfouhaily et al.* [2002], where it was demonstrated that a first order relationship exists between the moments of the DDM and the full set of  $DMSS_\lambda$  if the impact of the bistatic WAF and antenna gain are neglected:  $MSS = \lambda^2 B^2 / (2V^2 \sin^2 \epsilon)$ , where  $\epsilon$  is the transmitter elevation,  $V$  the receiver speed and  $B$  the DDM Doppler bandwidth. Assuming that the MSS did not vary significantly between the times of the ascending and descending passes and considering the relative velocity between sea-surface scatterers and aircraft, i.e.,  $V \pm v_s$  for the descending/ascending passes respectively, we can roughly solve for the scatterer velocity  $v_s$  (for simplicity assumed here parallel to the ground track). Applying this scheme to all possible pairs of measurements and averaging, the plot of Figure 3 results. The apparent mean scatterer velocity variations correlate with the JASON-1 wind speed variations. Moreover, from the dispersion relation an average scatterer speed of 8 m/s corresponds to waves of about 45 m wavelength. The detected motion thus seems to be associated with the longer and more coherent wave components, consistent with optical observations of the swell vector (wavelength and direction, see *Soulat* [2003]), revealing the presence of a northerly (almost aligned with the flight track) generated 48 m wave system. As hypothesized, the quasi-specular facets contributing the most to the bistatic reflected signals may, on average, be assumed to almost coherently travel with the dominating longer wave peak component.

## 5. Conclusion

We have reported the inversion of GNSS-R signals using, for the first time, the full Delay-Doppler Maps for the retrieval of the sea-surface directional mean square slope,  $DMSS_\lambda$ : the estimates show good inter-PRN consistency (except for the measured anisotropy SPI) and fair agreement with other sources of data.

The use of the full DDM further has helped to reveal a geophysical signature in GNSS-R associated with the mean sea surface scatterer velocity. Under quasi-specular conditions, sea surface scatterers are mostly associated to small slopes corresponding to longer waves with velocities that can reach 5-10 m/s, impacting significantly the Doppler bandwidth of slow-moving receivers (e.g., airborne or ground-based, *Soulat* [2004]). The detection of such a geophysical signature opens new opportunities for GNSS-R speculometry: to infer either  $DMSS_\lambda$  or a combination of  $DMSS_\lambda$  and scatterer velocity, depending on the aircraft speed. Further investigations will be carried out to take into account the correct deformation of the Doppler lines on the surface for the search of a scatterer velocity vector. Finally, we emphasize that the flight was not optimized for speculometry: higher and faster flights are needed in the future to consolidate the DDM inversion technique and to test new higher resolution inversion concepts.

**Acknowledgments.** The data analysis and the experimental campaign were respectively carried out under the ESA contracts 3-10120/01/NL/SF (OPPSCAT) and TRP-ETP-137.A. We thank the Institut Cartogràfic de Catalunya for flawless flight operations and aircraft GPS/INS kinematic processing. All Starlab authors have contributed significantly; the Starlab author list has been ordered randomly.

## References

- Armatys, M., A. Komjathy, P. Axelrad, and S. Katzberg. A comparison of GPS and scatterometer sensing of ocean wind speed and direction. In Proc. IEEE IGARSS, Honolulu, HA, 2000.
- Cardellach, E., G. Ruffini, D. Pino, A. Rius, A. Komjathy, and J. Garrison, Mediterranean balloon experiment: GPS reflection for wind speed retrieval from the stratosphere. *Rem. Sens. Env.*, 2003.
- Chelton, D.B., M.G. Schlax, M.H. Freilich, and R.F. Milliff, Satellite Measurements Reveal Persistent Short-Scale Features in Ocean Winds. *Science*, 303, Issue 5660, 978-983, 2004
- Elfouhaily, T., B. Chapron, K. Katsaros, and D. Vandemark, A unified directional spectrum for long and short wind-driven waves, *JGR*, 102(15):781-796, 1997.
- Elfouhaily, T., D. Thompson, and L. Linstrom, Delay-Doppler analysis of bistatically reflected signals from the ocean surface: Theory and application. *IEEE TGRS*, 40(3):560-573, 2002.
- Garrison, J.L., Katzberg, J.L., Effects of sea roughness on bistatically scattered range coded signals from the Global Positioning System, *GRL*, vol 25, n. 13, 1998.
- Garrison, J.L., Wind speed measurement using forward scattered GPS signals. *IEEE TGRS*, 40:50-65, 2002.
- Garrison, J.L., Anisotropy in Reflected GPS Measurements of Ocean Winds, in *Proceedings of the 2003 Workshop on Oceanography with GNSS-R*, Starlab, July 2003. Available at <http://starlab.es/gnssr2003/proceedings/>.
- Gourrion, J., D. Vandemark, S. Bailey, and B. Chapron, Investigation of C-band altimeter cross section dependence on wind speed and sea state, *Can. J. Rem. Sens.*, Vol. 28, No. 3, pp. 484-489, 2002.
- Komjathy, A., V. Zavorotny, P. Axelrad, G.H. Born, and J.L. Garrison, GPS signal scattering from sea surface: Wind speed retrieval using experimental data and theoretical model. *Rem. Sens. Env.*, 73:162-174, 2000.
- Ruffini, G., J.L. Garrison, E. Cardellach, A. Rius, M. Armatys, and D. Masters. Inversion of GPS-R delay-Doppler mapping waveforms for wind retrieval. In Proc. IEEE IGARSS, Honolulu, HA, 2000.
- Ruffini, G., F. Soulat, M. Caparrini, O. Germain and M. Martin-Neira, The Eddy Experiment I: Accurate GNSS-R ocean altimetry from low altitude aircraft, to appear in *GRL*, 2004.
- Soulat, F., Sea surface remote-sensing with GNSS and sunlight reflections, *Doctoral Thesis*, Universitat Politècnica de Catalunya/Starlab, 2003. Available at <http://starlab.es/library.html>.
- Soulat, F., M. Caparrini, O. Germain, P. Lopez-Dekker, M. Taani, G. Ruffini, Sea state monitoring using coastal GNSS-R, submitted to *GRL*, <http://arxiv.org/abs/physics/0406029>.
- Watson W. G., et al., NASA/GODDARD Research Activities for the Global Ocean Carbon Cycle: A Prospectus for the 21st Century, December 99.
- Zavorotny V., and A. Voronovich, Scattering of GPS signals from the ocean with wind remote sensing application, *IEEE TGRS*, 38(2):951-964, 2000.
- Zuffada, C., and T. Elfouhaily, Determining wind speed and direction with ocean reflected GPS signals, In *Sixth Int. Conf. on Rem. Sens. for Marine and Coastal Environments*, Charleston, 2000.